

Structure of the Convective Boundary Layer and Measurements of Areally Averaged Heat Flux

R. L. Coulter
Argonne National Laboratory
Argonne, Illinois

Introduction

Past efforts (Coulter et al. 1993, 1995) have shown that measurements of vertical velocity, w , in coherent structures within the Planetary Boundary Layer (PBL) in convective conditions can be directly related to the convective velocity scale, w^* , which is, in turn, related to areally averaged heat flux, H , and the mixed-layer height, z_i .

Analysis of data from the Boardman ARM Regional Flux Experiment (BARFEX) in 1992 (Doran et al. 1992) and an Intensive Operating Period (IOP) at the central facility of the Southern Great Plains Cloud and Radiation Testbed (CART) during October 1994 (IOP94) indicated that $w^* = \alpha w_i(0.5z_i)$, where w_i is the vertical velocity measured within thermal plumes, and α is a constant near 1.0. The definition of the boundaries of the thermal plumes is critical for the definition of w_i ; both the conditional sampling methods (used for the BARFEX data) and the wavelet transform methods (Coulter and Li 1995) used for IOP94 data rely on subjective determinations of controlling parameters such as threshold vertical velocity, plume length, and critical scale size.

The earlier approaches used measurements of the upward motion within the thermal plumes in parameterizations. This paper reports on results that instead use the downward motion of the vertical velocity field. In unstable conditions, the negative field results from forcing by the field of thermal plumes; downward motion should be a better estimate of the convective velocity field because 1) it is, in effect, an integral measure resulting from the field of thermals and 2) there is generally a preponderance of downward motion to compensate for the relatively strong, local thermal plumes, thus rendering more robust statistical characterization.

Discussion

Figure 1 shows the vertical velocity measured with the 915-MHz wind profiler 500 m above the central facility on 10 July 1995, between 0800 and 1600 CST. It is apparent

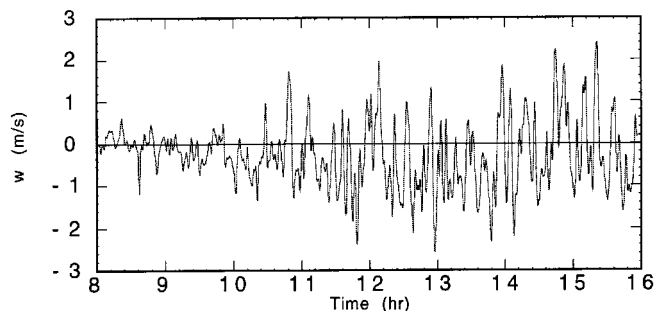


Figure 1. Time series of vertical velocity 500 m above the surface at the central facility on 10 July 1995 measured with the 915-MHz wind profiler. Data are 15-s averages, passed through 25-weight binary filter ($\overline{w_m} = -0.25$ m/s).

that the measured mean vertical velocity, $\overline{w_m}$, throughout this period is nonzero. Throughout IOP95 (26 June - 16 July 1995), $\overline{w_m}$ was predominantly negative between 0800 and 1600. Furthermore, the behavior illustrated in Figure 1, in which $\overline{w_m}$ becomes more negative during the middle portion of the day, is typical. This characteristic of the convective velocity field can be understood by realizing that within a field of coherent structures, the vertical velocity field is not homogeneous. It consists of spatially separated well-defined regions of vigorously rising air surrounded by descending air (Stull 1989; Ferrare et al. 1991); however, over a sufficiently large area,

$$\overline{w} = \iint w(x,y) dx dy = 0 \quad (1)$$

With any vertically pointing, stationary remote sensing device,

$$\overline{w_m} = \int w(x,y,t) dt \quad (2)$$

where the wind direction is along the x direction and $x = st$, where s is the horizontal wind speed and t is time. If one assumes that the horizontal cross section of a thermal plume is circular (measurements indicate that they are, in fact, slightly elliptical [Ferrare et al. 1991]), and if a square region

surrounding a thermal plume can be found within which (1) is true (Figure 2), then, assuming a mean rising velocity \bar{w}_+ and mean descending velocity \bar{w}_-

$$\bar{w}_+ = - \left(\frac{4}{\pi} \left(\frac{1}{d} \right)^2 - 1 \right) \bar{w}_-, \frac{1}{d} = \left(\frac{n_-}{n_+} \right)_{\min} + 1 \quad (3)$$

where n_- and n_+ are the number of negative and positive measured values of w , respectively, during the calculation of (2), $()_{\min}$ refers to the minimum possible value of the ratio, and the second part of (3) is only true for the case where the measurement axis passes through the center of the thermal. To apply this simple picture to the data from IOP95, we assume that a “composite” thermal, defined by the sum of all of the thermals that pass over the profiler during an averaging period (1 hr) also has the shape shown in Figure 2. This assumption is not generally true; however, it provides a useful conceptual basis for relating the negative velocity field to the positive velocities in thermals. On the basis of our observations, we have estimated $(n_-/n_+)_{\min}$ to be 0.5; thus $(l/d) = 1.5$, and

$$\bar{w}_+ = -1.86\bar{w}_- \quad (5)$$

A single realization of \bar{w}_m is defined by that portion of the composite thermal that passes over the profiler. When \bar{w}_+ and \bar{w}_- are constant, (2) is readily evaluated:

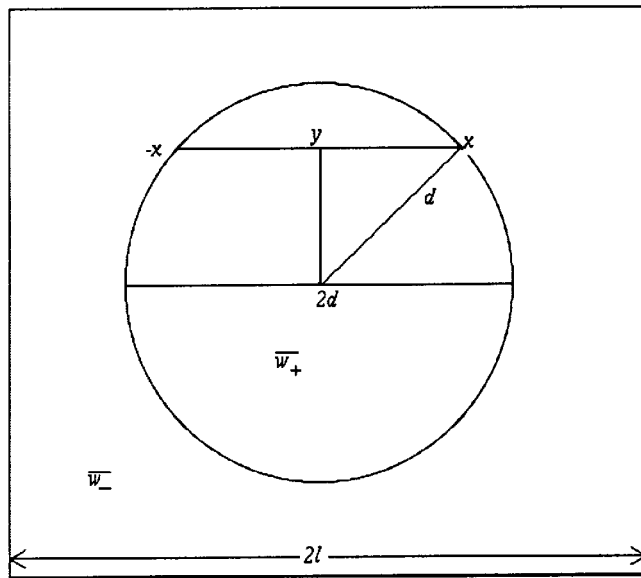


Figure 2. Geometry and definitions for area containing a circular thermal plume of radius d . Mean vertical velocity within rectangle is zero.

$$\begin{aligned} \bar{w}_m &= \bar{w}(1-\hat{x}) \\ &= \bar{w}_- \left(1 - \hat{i}^{-1} (1 - \hat{y}^2)^{1/2} \right) + \bar{w}_+ \hat{i}^{-1} (1 - \hat{y}^2)^{1/2} \end{aligned} \quad (5)$$

where

$$\hat{i} = \frac{l}{d}, \hat{x} = \frac{x}{d}, \hat{y}^2 = \left(\frac{y}{d} \right)^2 = \left[\frac{\hat{i}}{1 + (n_-/n_+)} \right]^2$$

In reality, of course, the vertical velocity field is not constant within a thermal. A number of different forms for the in-thermal field can be chosen [$w_i(r) = A(1-r^2/d^2)$, for example]. Figure 3 shows example fits for these functions using all the data from IOP95. Figure 1 shows that the negative velocity field is also not likely to be constant, as has been assumed. A similar form can be assumed for the negative field; however, these forms are less than satisfactory because they are not continuous at $r = d$. We can use a continuous definition for the w field of the form

$$w(r) = \frac{w_1}{(1-\alpha r^2)^k} - w_2 \quad (6)$$

where k can be $1/2, 1, 3/2, 2$, etc., and α is defined such that $w(d) = 0$. Then w at the center of the plume is $w_1 - w_2$, and the maximum negative value is $w(l)$. Table 1 shows comparative values and fits to the data for different forms of $w(r)$.

Thus, several forms are available for describing the spatial variation of the vertical velocity field that fit the data reasonably well, yet a large variation exists in the associated mid-thermal and maximum negative velocities.

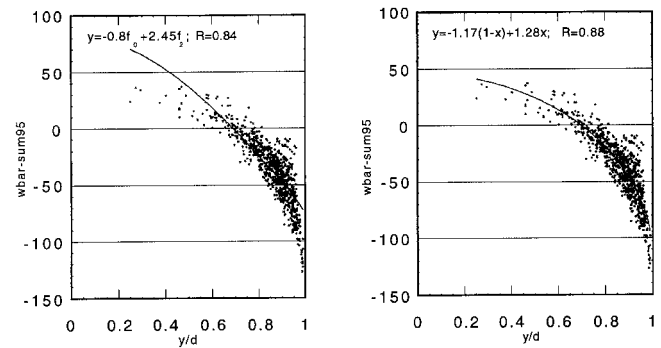


Figure 3. Measured \bar{w}_m versus calculated y/d ; left curve fit is for w_+ assumed constant, and right curve fit assumes equation $\bar{w}_+ = A(1-r^2/d^2)$.

Table 1. Different forms for $w(r)$ and associated values of mid-thermal (w_c), edge ($w_e = w(l)$) and regression of fit to all available data from IOP95.

Form for $w(r)$	w_c (m/s)	w_e (m/s)	R
both const	1.28	-1.77	0.77
$w_+(1-r^2)$	1.99	-0.61	0.70
w_+, w_- as	2/48	-1.11	0.69
$A_+(1-r^2)$			
$k=.5$ Eq (6)	3.13	-0.78	0.66
$k=1$ Eq (6)	3.04	-1.09	0.66
$k=2$ Eq (6)	4.29	-0.97	0.64

Nevertheless, the best fit to the overall data set is obtained when the thermal positive velocity field is assumed to be constant. All analyses that assumed that the thermal upward motion decreased with distance from the center overestimated $\overline{w_m}$ for small (n/n_+). Obviously, this is not what is to be expected for individual thermals; however, when an “average” is calculated over a relatively long time, several thermals will be sampled, and each thermal will be intersected at a different location. This has the effect of “smearing” the spatial distribution of thermal velocities; for example, if the center of one thermal passes over the profiler and if the edge of another identical thermal passes over during the same averaging interval, the “composite” thermal will be relatively uniform.

Results

The cumulative probability distribution for w indicates that $\overline{w_m}$ is positive in about 9% of the cases. On the other hand it is clear from Figure 2 that $\overline{w_m}$ is positive when $y < .07d$, and one would expect $\overline{w_m} > 0$ in about 50-70% of the cases (all values of y are equally likely). This implies that the shape of the composite thermal must be as in Figure 4, with small values of n/n_+ likely to occur less often than otherwise.

Figure 5 compares values of w_t calculated with (4) (where $\overline{w_-}$ is determined by averaging the negative velocity profile between 200 m and $0.6 z_i$) with w^* determined either locally at the central facility or averaged over 10 Bowen ratio stations over the CART site. In both cases, z_i was determined subjectively from vertical time sections of signal strength measured by the 915-MHz profiler at the central facility. It is evident that the agreement is better with average w^* , as was observed with the IOP94 data (Coulter et al. 1995). This is probably because the average w^* values represent a better statistical sample of the variation of surface likely to affect the

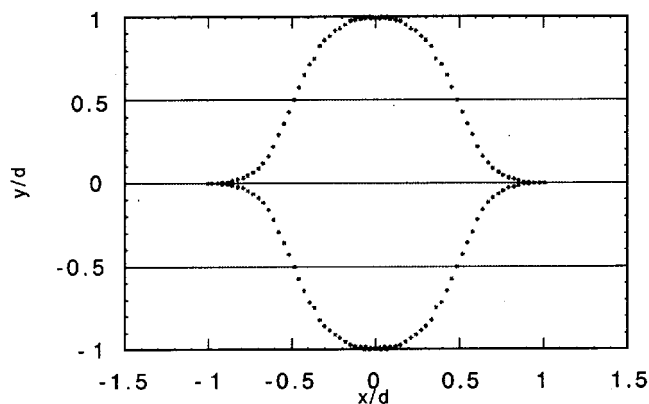


Figure 4. Diagram of actual “composite” thermal shape, calculated by equating the cumulative probability of w with y/d and calculating x/d from Figure 4. Diagram of actual “composite” thermal shape, calculated by equating the cumulative probability of w with y/d and calculating x/d from (n/n_+) .

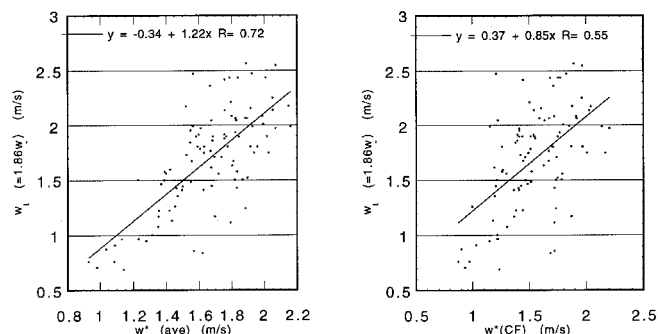


Figure 5. Scatter plots of derived w^* versus w^* calculated from surface measurements and z_i . Left plot uses values of w^* averaged over the CART site; right uses central facility only.

PBL development within 10 km of the central facility than is obtained from the flux measurements over the central facility alone. When the positive portions of the velocity field are used, the regression value is 0.53.

Furthermore, a better agreement with the data is achieved if

$$w_t = \overline{w_+} = 1.52\overline{w_-} + 0.277 \quad (7)$$

is used instead of (4). This observation is further corroboration that the “shape” of the composite thermal is not circular. Integration of the shape of Figure 5 predicts a coefficient of 1.67 for (7).

When the data from Figure 5 are stratified by time of day (Figure 6), it is clear that the relationship between w_i and w^* is better defined before, rather than after, noon. This may just be a result of the larger differences usually encountered before noon as both the sensible heat flux and the mixed layer increase rapidly; or it may be the result of inappropriate averaging times used during the afternoon, as the thermal plumes become too large to obtain sufficient samples to attain significance within an hour.

By using the calculated values of w_i with (7), we can estimate areally averaged surface sensible heat flux can be calculated, using z_i and w^* from profiler data. Values calculated from selected days during IOP95 are shown in Figure 7. Clearly, the method gives reasonable values and exhibits expected daily variations; however, because the calculated H is proportional to the third power of w^* , small errors in w^* can lead to large errors in calculated H . We are working to develop methods to ameliorate this problem while maintaining the theoretical basis of the calculations.

References

Coulter, R.L., T.J. Martin, D.R. Cook, T.A. Tyce, and D.L. Brandner, 1993: Intensity and Vertical Velocity Profiles over Varying Surface Types and their Relationship to Areal Average Heat Flux. In *Preprints, Fourth Symposium on Global Change Studies, 73rd American Meteorological Society Annual Meeting*, 17-22 Jan. 1993, Anaheim, California, pp. 152-156. American Meteorological Society, Boston, Massachusetts.

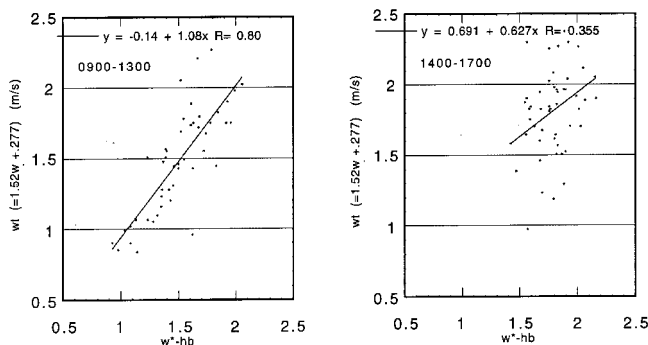


Figure 6. Plots of calculated w^* using equation (7) for before and after noon.

Coulter, R.L., T.J. Martin, and D.J. Holdridge, 1995: Using remotely sensed planetary boundary layer variables as estimates of areally averaged heat flux. In *Proceedings of the Fifth Atmospheric Radiation Measurement (ARM) Science Team Meeting*, 3-6 March 1995, San Diego, California. CONF-9503140, U.S. Department of Energy, Washington, D.C.

Coulter, R.L., and B.L. Li, 1995: A technique using the wavelet transform to identify and isolate coherent structures in the planetary boundary layer. In *Proceedings, 11th Symposium on Boundary Layers and Turbulence*, 27-31 March, Charlotte, North Carolina. American Meteorological Society, Boston, Massachusetts.

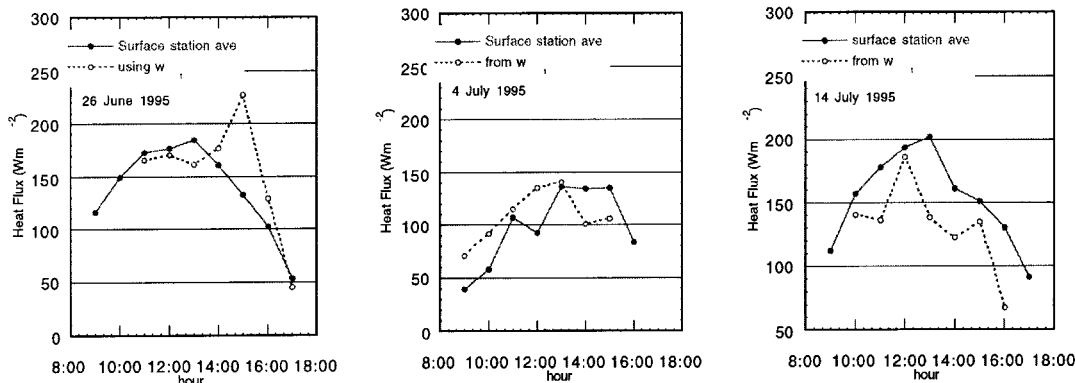


Figure 7. Values of H calculated by using estimates of midthermal velocities as measures of the convective velocity scale compared with average Bowen ratio estimates of H averaged over the CART site.

Doran, J.C., F.J. Barnes, R.L. Coulter, T.L. Crawford, D.D. Baldocchi, D.R. Cook, D. Cooper, R.J. Dobosy, L. Fritschen, R.L. Hart, L. Hipps, J.M. Hubbe, W. Gao, R.R. Kirkham, K.E. Kunkel, T.J. Martin, T.J. Meyers, W. Porch, J.D. Shannon, W.J. Shaw, E. Swiatek, and C.D. Whiteman, 1992: The Boardman Regional Flux Experiment, *Bull. Am. Meteorol. Soc.*, **73**, 1785-1795.

Ferrare, R.A., J.L.Schols, E.W. Eloranta, and R.L. Coulter, 1991: Lidar Observation of Banded Convection During BLX83. *J. Appl. Meteorol.* **30**, 312-326.

Stull, R.B, 1989: *An Introduction to Boundary Layer Meteorology*, Kluwer Academic Publishers, Boston, Massachusetts.